Spectrochimica Acta Part A 94 (2012) 126–133

Contents lists available at SciVerse ScienceDirect

Spectrochimica Acta Part A: Molecular and Biomolecular Spectroscopy

journal homepage: www.elsevier.com/locate/saa

Synthesis, FT-IR, FT-Raman, dispersive Raman and NMR spectroscopic study of a host molecule which potential applications in sensor devices

M. Kurt[a,*], M. Karabacak[b], S. Okur[c], S. Sayin[d], M. Yilmaz[d], N. Sundaraganesan[e]

[a] Department of Physics, Ahi Evran University, 40100 Kırşehir, Turkey
[b] Department of Physics, Afyon Kocatepe University, 03040 Afyonkarahisar, Turkey
[c] Faculty of Engineering and Architecture, Izmir Katip Celebi University, Izmir, Turkey
[d] Department of Chemical, Selcuk University, Selcuklu, Konya, Turkey
[e] Department of Physics (Engg.), Annamalai University, Annamalai Nagar, Chidambaram 608002, Tamil Nadu, India

ARTICLE INFO

Article history:
Received 8 February 2012
Received in revised form 18 March 2012
Accepted 21 March 2012

Keywords:
FT-IR
FT-Raman
Dispersive Raman
NMR
DFT

ABSTRACT

The solid phase FT-IR, FT-Raman and dispersive Raman spectra of the host molecule which potential applications in sensor devices have been recorded in the region 400–4000 and 50–3500 cm^{-1}, respectively. The spectra were interpreted in terms of fundamentals modes, combination and overtone bands. The structure of the molecule was optimized and the structural characteristics were determined by density functional theory (DFT) using B3LYP method with 6-31G(d) basis set. The vibrational frequencies were calculated for the studied molecule by DFT method, and compared with the experimental frequencies, which yield good agreement between observed and calculated frequencies. Finally the calculation results were applied to simulate infrared and Raman spectra of the compound. Obtained these spectra also showed good agreement with observed spectra. The dipole moment, linear polarizability and first hyperpolarizability values were also computed. The linear polarizability and first hyperpolarizability of the studied molecule indicate that the compound is a good candidate of nonlinear optical materials.

1. Introduction

Molecular recognition plays an extremely important role in chemistry and biochemistry, especially in the fast growing field of supramolecular host–guest chemistry [1,2]. One interesting class of supramolecular systems is the macrocyclic calixarenes that are widely used as effective host compounds for various guest species such as cations, anions, and neutral molecules [3–6]. Calixarenes have been attracted much attention in supramolecular chemistry due to the application in enzyme mimics, host–guest chemistry, selective ion transport, and sensors [6–9]. One of the most important features of these compounds is their diversity. The most well known member of this class is calyx(4)arene which comprises cyclic tetramers of phenol units linked by ortho-methylene bridges and reveals a basket-shaped molecular structure [10].

In a previously work, Suwattanamala et al. [11] have made computational study of calyx(4)arene derivatives and complexation with Zn^{+2}. Kim et al. [12] have investigated the DFT conformational study of Calix(5)arene and Calix(4)arene. Ab initio studies of NMR chemical shifts for calyx(4)arene and its derivatives have been done by Kara et al. [13]. Cao et al. [14] have studied the B3LYP and MP2 theoretical investigation into host–guest interaction between calyx(4)arene and Li^+ or Na^+. Liu et al. [15], synthesised and investigated crystal structure of 26,28-bis(cyanomethoxy)-25,27-dihydroxycalix[4]arene. Azo-functionalized calix[4]arenes and were synthesised and their application to chlorideselective electrode as ionophores were searched by Lee et al. [16]. Bayrakci et al. [17] synthesised of p-tert-butylcalix[4]arene b-ketoimin derivatives for extraction of dichromate anion. To our knowledge, no attempts to theoretically assign the experimental vibrational spectra of 5,11,17,23-Tetra-p-tert-butyl-25,27-bis[aminoethyl]-26-28 dihydroxycalix[4]arene have been done yet.

In the present work, molecular structure and vibrational spectra of 5,11,17,23-Tetra-p-tert-butyl-25,27-bis[aminoethyl]-26-28 dihydroxycalix[4]arene molecule have been investigated. The theoretically predicted values have been compared with the experimentally measured data and also the results have been discussed. Nowadays, the progress of various theoretical methods has made possible the calculation of vibrational potential fields of large size molecules with moderate computational effort. Organic molecules which are able to manipulate photonic signals efficiently are of importance in technologies such as optical communication, optical computing, and dynamic image processing [18,19].

* Corresponding author. Tel.: +90 386 211 45 54.
E-mail addresses: kurt@gazi.edu.tr, mkurt@ahievran.edu.tr (M. Kurt).

1386-1425/$ – see front matter.
http://dx.doi.org/10.1016/j.saa.2012.03.070

2. Experimental

2.1. Synthesis of 5,11,17,23-Tetra-p-tert-butyl-25,27-bis[cyanomethoxy]-26-28-dihydroxycalix[4]arene (**2**) and 5,11,17,23-Tetra-p-tert-butyl-25,27-bis[aminoethyl]-26-28 dihydroxycalix[4]arene (**3**)

2.1.1. 5,11,17,23-Tetra-p-tert-butyl-25,27-bis[cyanomethoxy]-26-28-dihydroxycalix[4]arene (**2**)

p-Tert-butylcalix-[4]arene (**1**) (6.5 g, 10.03 mmol), K_2CO_3 (8.53 g, 61,81 mmol), chloroacetonitrile (4.2 ml, 0.03 mol) and NaI (9.25 g, 61.66 mmol) was refluxed in dry acetone (250 mL) for 7 h. The cooled mixture was filtered, than washed with CH_2Cl_2. The filtrate was evaporated under reduced pressure, 40 ml anhydrous ethanol was added to produce a white precipitate. The white precipitate was removed by filtration and recrystallized from anhydrous acetone to give pure white crystals of compound 2 (yield: 3.99 g, 53%; mp: 242–245 °C; IR (KBr) 2247 cm^{-1} (CN); ^1H NMR ($CDCl_3$) δ (ppm): 0.87 (s, 18H, Bu^t), 1.32 (s, 18H, Bu^t), 3.42 (d, 4H, $ArCH_2Ar$), 4.22 (d, 4H, $ArCH_2Ar$), 4.79 (s, 4H, OCH_2CN), 5.52 (s, 2H, ArOH), 6.72 (s, 4H, ArH), 7.11 (s, 4H, ArH), Anal. calculated for $C_{48}H_{58}N_2O_4$: C, 79.30%; H, 8.04%; N, 3.85%. Found: C, 79.51%; H, 8.25%; N, 3.53%.

2.1.2. 5,11,17,23-Tetra-p-tert-butyl-25,27-bis[aminoethyl]-26-28-dihydroxycalix[4]arene (**3**)

5,11,17,23-Tetra-p-tert-butyl-25,27-bis[cyanomethoxy]-26-28 dihydroxycalix[4]arene (**2**) (1 g, 1.38 mmol) was solved and hard mixing in 50 ml diethylether. After $LiAlH_4$ (0.43 g, 11.3 mmol) was slowly added in mixture and refluxed for 5 h. The reaction flask was placed in ice bath and added 50 ml benzene and 2 ml water on the mixture carefully. The organic phase was filtered and The filtrate was evaporated under reduced pressure. In this way, the title compound which shown in Scheme 1 was synthesized. Yield: 0.90 g 79%, m.p: 143–145 °C. ^1H NMR ($CDCl_3$) δ (ppm): 1.01 (s, 18H, Bu^t), 1.25 (s, 18H, Bu^t), 3.30 (*t*, 4H, $-CH_2NH_2$), 3.38 (d, 4H, $ArCH_2Ar$), 4.08 (*t*, 4H, $-CH_2CH_2$), 4.33 (d, 4H, $ArCH_2Ar$), 6.96 (s, 4H, ArH), 7.05 (s, 4H, ArH), Anal. calculated for $C_{52}H_{76}N_2O_5$: C, 77.18%; H, 9.47%; N, 3.46%. Found: C, 77.34%; H, 9.65%; N, 3.21%.

2.2. FT-IR and FT-Raman measurements

The FT-IR spectrum of synthesized sample were measured with a KBr disc technique because of solid state. The IR spectrum of molecule was recorded in the region 400–4000 cm^{-1} on a Perkin Elmer FT-IR BX spectrometer calibrated using polystyrene bands. The FT-Raman spectrum of the sample was recorded using 1064 nm line of Nd:YAG laser as excitation wave length in the region 50–4000 cm^{-1} on a Bruker RFS 100/S FT-Raman. The detector is a liquid nitrogen cooled Ge detector. Five hundred scans were accumulated at 4 cm^{-1} resolution using a laser power of 100 mW.

3. Computational details

The entire calculations were performed at B3LYP level on Pentium IV personal computer using Gaussian 09 program package, involving gradient geometry optimization [20–22]. Initial geometry generated standard geometrical parameters minimized without any constraint in the potential energy surface at B3LYP level, adopting the 6-31G(d) basis set. The vibrational modes were assigned by means of visual inspection using the Gauss View program [23]. The symmetry of the molecule was also helpful in making vibrational assignments. The vibrational assignments of the normal modes were made on the basis of the TED calculated by using the VEDA 4 program [24]. Subsequent total energy distribution (TED) to each observed frequencies, predicts well the purity of the fundamental modes and shows the reliability and accuracy of the spectral analysis. The graphical presentation of the calculated Raman and IR spectra were made using Gauss View program [25]. The absence of imaginary frequency modes for the optimized structure of title molecule at DFT level confirms a true minimum on the potential energy surface. All the parameters were allowed to relax and all the calculations converged to an optimized geometry. Moreover, the dipole moment, nonlinear optical (NLO) properties, chemical hardness have also been studied using B3LYP/6-31G(d).

3.1. Prediction of Raman intensities

The Raman activities (S_{Ra}) calculated with Gaussian 09 program [20] converted to relative Raman intensities (I_{Ra}) using the following relationship derived from the intensity theory of Raman scattering [25,26].

$$I_i = \frac{f(\nu_0 - \nu_i)^4 S_i}{\nu_i[1 - \exp(-hc\nu_i/kT)]}$$

where, ν_0 is the laser exciting wavenumber in cm^{-1} (in this work, we have used the excitation wavenumber $\nu_0 = 9398.5\ cm^{-1}$, which corresponds to the wavelength of 1064 nm of a Nd:YAG laser), ν_i the vibrational wavenumber of the *i*th normal mode (cm^{-1}), while S_i is the Raman scattering activity of the normal mode ν_i. f (is a constant equal to 10^{-12}) is a suitably chosen common normalization factor for all peak intensities. h, k, c and T are Planck and Boltzmann constants, speed of light and temperature in Kelvin, respectively.

4. Results and discussion

4.1. Molecular geometry

The optimized molecular structure of studied molecule belongs to C_1 point group symmetry. The optimized geometry is performed at B3LYP/6-31G(d) basis set of the studied molecule with atom numbering scheme is shown in Fig. 1. The optimized structural parameters such as bond lengths and bond angles are presented in Tables 1a and 1b. The molecular structure is not planar. However, the OH groups were found to be planar with benzene rings. In one point of view, the molecule appears like chair form. The atoms are closely packed due to the intramolecular hydrogen bonding. It is evident from the bond length values of O63—H66 = 1.835 Å and O61—H62 = 0.975 Å as shown in Table 1a). The C—O bond length attached with the hydroxyl group is smaller than the C—O bond length attached with the $-CH_2-CH_2-NH_2$ group. It is evident from the table, C1—O65 = 1.362 Å, C23—O61 = 1.361 Å are smaller values and C12—O63 = 1.406 Å, C73—O63 = 1.446 Å, C34—O64 = 1.385 Å, C67—O64 = 1.431 Å are larger values. Some of the bond angles are deviated from the co-planarity due to the charge transfer interaction between the atoms in the hydrogen bonded molecule.

4.2. Vibrational assignments

Vibrational spectroscopy is one of the most useful experimental tools for study of hydrogen bonded complexes. Therefore, the information obtained from calculated harmonic vibrational frequencies can be useful. In our present study, we have performed a frequency calculation analysis to obtain the spectroscopic signature of title molecule. The studied molecule consists of 84 atoms therefore they have 246 vibrational normal modes. All the frequencies are assigned in terms of fundamental, overtone and combination bands. The recorded (FT-IR, FT-Raman and dispersive Raman with

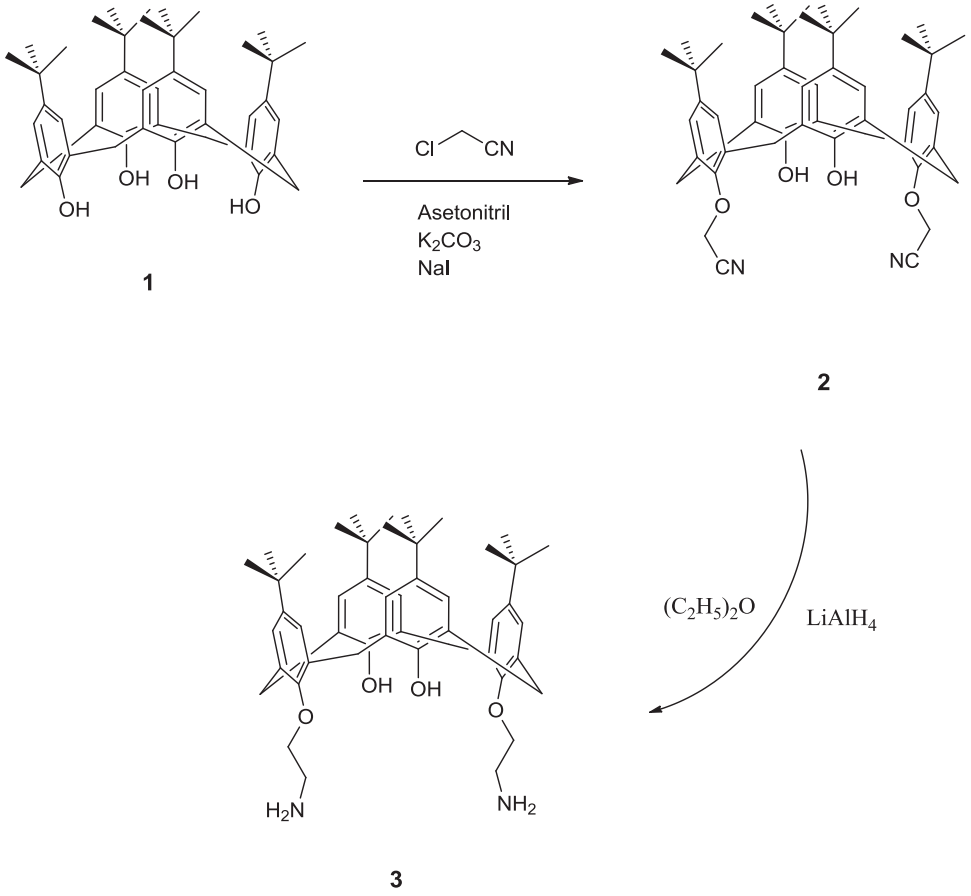

Scheme 1. Synthesis of 5,11,17,23-Tetra-p-tert-butyl-25,27-bis[aminoethyl]-26-28 dihydroxycalix[4]arene molecule.

different laser) and calculated vibrational wavenumbers along with their relative intensities and probable assignments with TED of the studied molecule are given in Table 2. The theoretical spectra were obtained from the B3LYP/6-31G(d) method using Lorentzian band shape with band width on half-height 10 cm^{-1}. This reveals good correspondence between theory and experiment in main spectral features. The experimental and theoretical spectra are shown in Fig. 2. The dispersive Raman spectra are shown in Figs. 3 and 4.

Table 1a
The calculated some selected bond lengths in angstrom (Å) and bond angles (°) of 5,11,17,23-Tetra-p-tert-butyl-25,27-bis[aminoethyl]-26-28 dihydroxycalix[4]arene molecule.

Bond lengths	B3LYP	Bond lengths	B3LYP	Bond angles	B3LYP	Bond angels	B3LYP	Bond angels	B3LYP
C1—C2	1.410	C1—O65	1.362	C2—C1—C8	120.7	H21—C20—C24	108.1	C2—C42—H43	109.6
C1—C8	1.405	C23—O61	1.361	C2—C1—O65	115.7	H22—C20—C24	109.9	C2—C42—H44	108.8
C2—C3	1.393	C12—O63	1.406	C8—C1—O65	123.5	C24—C23—C30	120.7	C41—C42—H43	109.4
C3—C5	1.403	C73—O63	1.446	C1—C2—C3	118.6	C24—C23—O61	123.5	C41—C42—H44	110.0
C5—C6	1.395	C34—O64	1.385	C2—C3—C5	122.2	C30—C23—O61	115.7	O64—C67—C68	112.9
C6—C8	1.402	C67—O64	1.431	C3—C5—C6	117.6	C23—C24—C25	118.4	O64—C67—H69	111.3
C12—C13	1.402	C5—C57	1.512	C5—C6—C8	122.4	C24—C25—C27	122.4	O64—C67—H70	105.4
C12—C19	1.401	C16—C53	1.511	C1—C8—C6	118.4	C25—C27—C28	117.6	C68—C67—H69	109.0
C13—C14	1.398	C27—C49	1.512	C8—C9—H10	109.8	C27—C28—C30	122.3	C68—C67—H70	110.0
C14—C16	1.399	C38—C45	1.512	C8—C9—H11	108.1	C23—C30—C28	118.4	C67—C68—H71	108.8
C16—C17	1.398	C2—C42	1.521	C8—C9—C13	114.1	C30—C31—H32	110.1	C67—C68—H72	108.9
C17—C19	1.399	C8—C9	1.524	H10—C9—C13	110.1	C30—C31—H33	108.7	H71—C68—N82	108.1
C23—C24	1.405	C9—C13	1.527	H11—C9—C13	108.2	C30—C31—C35	111.3	H72—C68—N82	114.6
C23—C30	1.410	C19—C20	1.527	C13—C12—C19	122.7	H32—C31—C35	108.9	O63—C73—C74	107.6
C24—C25	1.402	C20—C24	1.525	C13—C12—O63	118.5	H33—C31—C35	109.9	O63—C73—H77	109.0
C25—C27	1.395	C30—C31	1.520	C19—C12—O63	118.6	C35—C34—C41	120.5	O63—C73—H78	109.9
C27—C28	1.403	C31—C35	1.527	C9—C13—C12	122.4	C35—C34—O64	119.3	C74—C73—H77	111.4
C28—C30	1.393	C41—C42	1.529	C9—C13—C14	120.1	C41—C34—O64	120.1	C74—C73—H78	110.7
C34—C35	1.407	C67—C68	1.530	C12—C13—C14	117.4	C31—C35—C34	122.0	C73—C74—H75	108.6
C34—C41	1.409	C73—C74	1.525	C13—C14—C16	122.0	C31—C35—C36	119.4	C73—C74—H76	109.0
C35—C36	1.399	C68—N82	1.468	C14—C16—C17	118.4	C34—C35—C36	118.5	H75—C74—N79	108.6
C36—C38	1.396	C74—N79	1.465	C16—C17—C19	122.0	C35—C36—C38	122.2	H76—C74—N79	115.0
C38—C39	1.397	O63—H62	1.841	C12—C19—C17	117.4	C36—C38—C39	117.7	C74—N79—H80	110.1
C39—C41	1.398	O63—H66	1.835	C19—C20—H21	108.2	C38—C39—C41	122.2	C74—N79—H81	109.9
O65—H66	0.975	O61—H62	0.975	C19—C20—H22	110.1	C34—C41—C39	118.4	C68—N82—H83	109.9
				C19—C20—C24	114.1	C2—C42—C41	111.1	C68—N82—H84	109.7

Table 1b
The calculated some average bond lengths in angstrom (Å) and bond angles (°) of 5,11,17,23-Tetra-p-tert-butyl-25,27-bis[aminoethyl]-26-28 dihydroxycalix[4]arene molecule.

Bond lengths	B3LYP	Bond angles	B3LYP
(C—H) methyl	1.097	(H—C—H) methyl	107.4
(C—H) methylene	1.096	C_{ring}—(C—H) methyl	111.5
(C—H) benzene	1.089	(C—C—H) ring	118.9
(N—H) amino	1.018	(H—C—H) methylene	107.2
		$(C—C)_{ring}$—$(C)_{methyl}$	121.1
		(H—N—H) amino	106.1
		C—O—H	112.5
		C—C—N	109.0
		C—O—C	116.1
		$(C—C)_{ring}$—$(C)_{methylene}$	120.8

The computed vibrational wavenumbers and the atomic displacements corresponding to the different normal modes are used for identifying the vibrational modes unambiguously. The calculated wavenumbers are usually higher than the corresponding experimental quantities, due to the combination of electron correlation effects and basis set deficiencies. After applying, the scaling factor, the theoretical wave numbers are in good agreement with experimental wavenumbers. In our present work, the calculated frequencies are scaled by 0.9603 for B3LYP with 6-31G(d) method.

4.2.1. C—H vibrations

The existence of one or more aromatic rings in a structure is normally readily determined from the C—H and C=C—C ring related vibrations. The substituted benzene like molecules give rise to C—H stretching, C—H in-plane and C—H out-of-plane bending vibrations. The aromatic structures show the presence of C—H stretching vibration in the region 3100–3000 cm^{-1}, which is the characteristic region for the ready identification of C—H stretching vibration [27,28]. In this region, the bands are not affected appreciably by the nature of the substituent. In our present work, the C—H stretching vibrations were observed at 3046(vw), 2953(s) cm^{-1} in FT-IR spectrum and at 3038(vw), 2959(s) and 2879(vw) cm^{-1} in FT-Raman spectrum for C—H vibrations. The same vibrations are observed at 3038(vw), 3035(vw), 2956(m), 2955(m), 2910(vw) and 2902(m) cm^{-1} in dispersive Raman spectra with different laser. The calculated values of these modes for the molecule were found in the range 3054–2862 cm^{-1} at the DFT-B3LYP calculation level. As indicated by the TED, these four modes involve above 95% contribution suggesting that they are pure stretching modes.

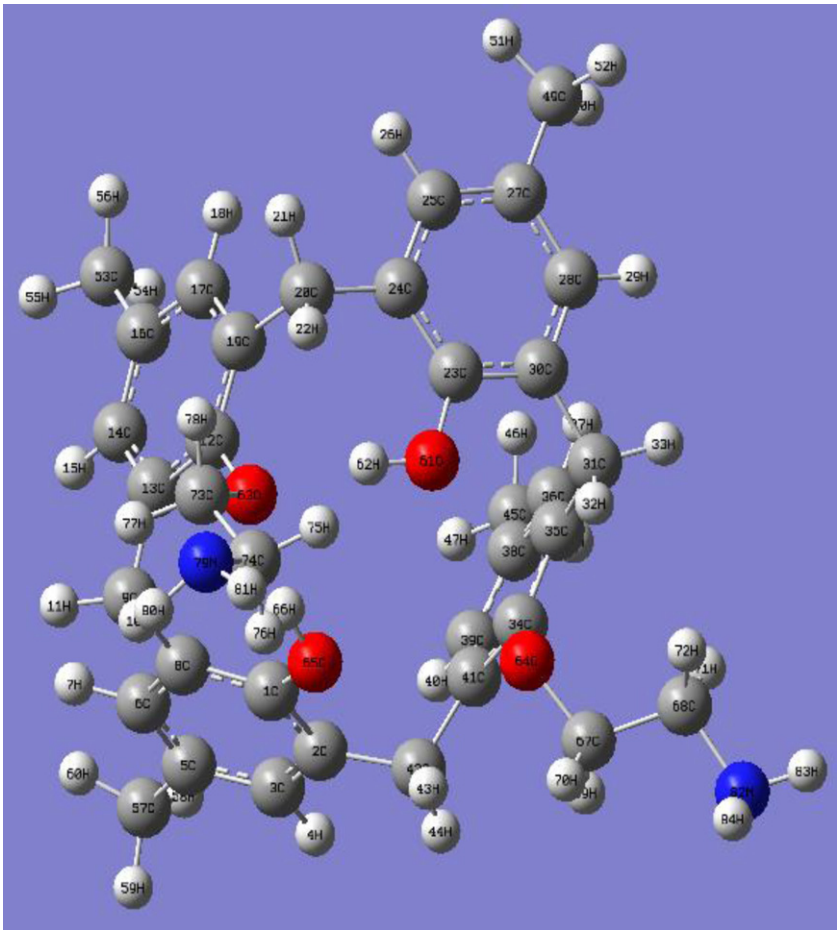

Fig. 1. Molecular structure and atom numbering of 5,11,17,23-Tetra-p-tert-butyl-25,27-bis[aminoethyl]-26-28 dihydroxycalix[4]arene molecule.

Table 2
Comparison of the selected calculated and experimental vibrational spectra and proposal assignments of 5,11,17,23-Tetra-p-tert-butyl-25,27-bis[aminoethyl]-26-28 dihydroxycalix[4]arene molecule.

Experimental					6-31G(d)/B3LYP				TED[c] (≥10%)
No	FT-IR	[a]DR (532 nm)	[a]DR (785 nm)	FT-Raman	Scaled[b]	I_{IR}	S_{Ra}	I_{Ra}	Assignments
6				40vw	40	0.81	0.81	0.02	Γ COCC (36) + Γ CCCC (14)
19		114s		124vs	118	2.28	0.42	0.00	Γ CCCC (29) + Γ CCCO (25)
20			127s		130	0.91	1.87	0.01	β CCC (44)
37			260vw	263w	264	1.81	2.17	0.01	β CCO (32) + ν CO (14) + β COC (11)
61				500vw	503	5.97	3.49	0.17	β CCC (25) + ν CC (17) + β CCO (10)
65				540vw	546	0.42	15.13	0.61	Γ CCCC (21) + Γ HOCC (10)
66	553w				551	0.58	2.79	0.11	β CCO (27)
70		579w			579	3.22	4.49	0.16	Γ CCCC (13) + β COC (10)
72			589w	585s	584	5.19	2.53	0.09	β CCC (11) + β CCO (11)
75	636w				628	92.62	3.22	0.09	Γ HOCC (83)
78				675m	686	0.59	6.73	0.16	β CCC (20)
79				699m	708	4.64	8.27	0.19	ν CO (25) + ν CC (24) + β CCC (10)
86	781vw				782	17.31	0.54	0.01	β CCH (30) + Γ HCCH (28) + Γ HNCH (23) + Γ COCH (11)
88		806w		814s	798	4.92	14.62	0.25	Γ CCCO (12) + ν CO (10) + β COC (10)
89	817vw		820w		838	14.73	3.93	0.06	Γ CCCH (62)
97	869s				872	1.10	1.07	0.01	Γ CCCH (50)
103		907w	916w	921m	918	2.57	3.33	0.04	ν CC (43)
106	944vw				943	5.37	11.23	0.13	ν CC (43) + β CNH (29) + ν CC (12) + β CCO (12) + ν CO (10) + β NCH (10)
114	998w				1000	2.80	1.98	0.02	β CCH (55) + ν CC (10)
119				1024vw	1032	1.15	1.11	0.01	β CCH (61) + Γ CCCH (18)
124		1044vw			1045	4.25	19.67	0.17	ν CN (77) + β NCH (14) + β CCO (10)
128				1111m	1111	55.69	2.80	0.02	ν CC (19) + ν CO (16) + β CCH (12)
129	1125m	1123w	1119w		1123	6.33	0.34	0.00	ν CC (20) + β CCH (14) + ν CO (10)
138			1195w		1187	95.20	0.90	0.01	β COH (37) + β CCH (17) + ν CC (16)
139	1199vs			1198m	1208	137.68	7.41	0.05	ν CO (33) + β CCH (27) + ν CC (10) + β CNH (10)
140		1213vw			1211	78.05	3.73	0.02	β COH (21) + β CCH (18) + ν CC (14)
141	1234w				1233	8.94	0.05	0.00	β CCH (29) + ν CO (10)
142				1238vw	1236	2.74	0.56	0.00	β CCH (48)
158				1302ms	1303	10.53	11.44	0.06	ν CC (41) + β CCH (16) + β COH (10)
159	1306w	1304w			1305	6.78	28.64	0.14	ν CC (39) + ν CO (17) + β CCH (10)
160			1312w		1311	0.66	15.61	0.08	ν CC (29) + β CCH (29)
164	1361ms				1343	2.27	1.43	0.01	β CNH (23) + β OCH (20) + β CCH (19) + β NCH (10)
168	1388vw				1387	1.09	61.64	0.26	β HCH (46) + β CCH (40)
175		1440w			1440	69.00	9.82	0.04	Γ CCCH (30) + β CHC (18)
177			1446w	1445s	1447	0.29	3.65	0.01	ν CC (13) + β HCH (10)
184	1461vw				1458	4.57	23.06	0.08	β HCH (54) + Γ CCCH (30) + β CCH (10)
193	1481vs				1483	3.22	2.61	0.01	β HCH (31) + Γ HCCH (19) + Γ HCCH (16) + Γ HCCO (10)
200	1596w				1595	12.36	25.92	0.07	ν CC (58) + β CH(19)
201		1603w		1603s	1601	0.07	23.02	0.07	ν CC (57)
202			1610w		1602	1.93	36.82	0.10	ν CC (56)
205				2879vw	2862	67.32	80.67	0.04	ν CH (96)
207		2902m	2910vw		2914	37.86	147.30	0.06	ν CH (98)
216					2942	35.55	134.52	0.05	ν CH (98)
217	2953s	2956m	2955m	2959s	2959	4.89	68.04	0.03	ν CH (98)
234			3035vw		3035	43.06	35.06	0.01	ν CH (98)
235		3038vw		3038vw	3037	11.22	89.11	0.03	ν CH (98)
237	3046vw				3046	22.28	25.35	0.01	ν CH (98)
241		3315vw		3328vw	3328	3.23	170.22	0.04	ν NH (99)
242	3358br				3342	0.63	145.26	0.03	ν NH (99)
243			3415vw		3411	0.18	105.46	0.02	ν NH (99)
245			3445w		3480	472.74	118.78	0.02	ν OH (99)

s, strong; m, medium; w, weak; vs, very strong; ms, medium strong; vw, very weak; br, broad; ν, stretching; β, in plane bending; Γ, torsion.
[a] Dispersive Raman
[b] Scale factor of 0.9603 was used for B3LYP/6-31G(d) basis set [frequency (cm^{-1}), intensities; I_{IR} ($K\,mmol^{-1}$)].
[c] Total energy distribution.

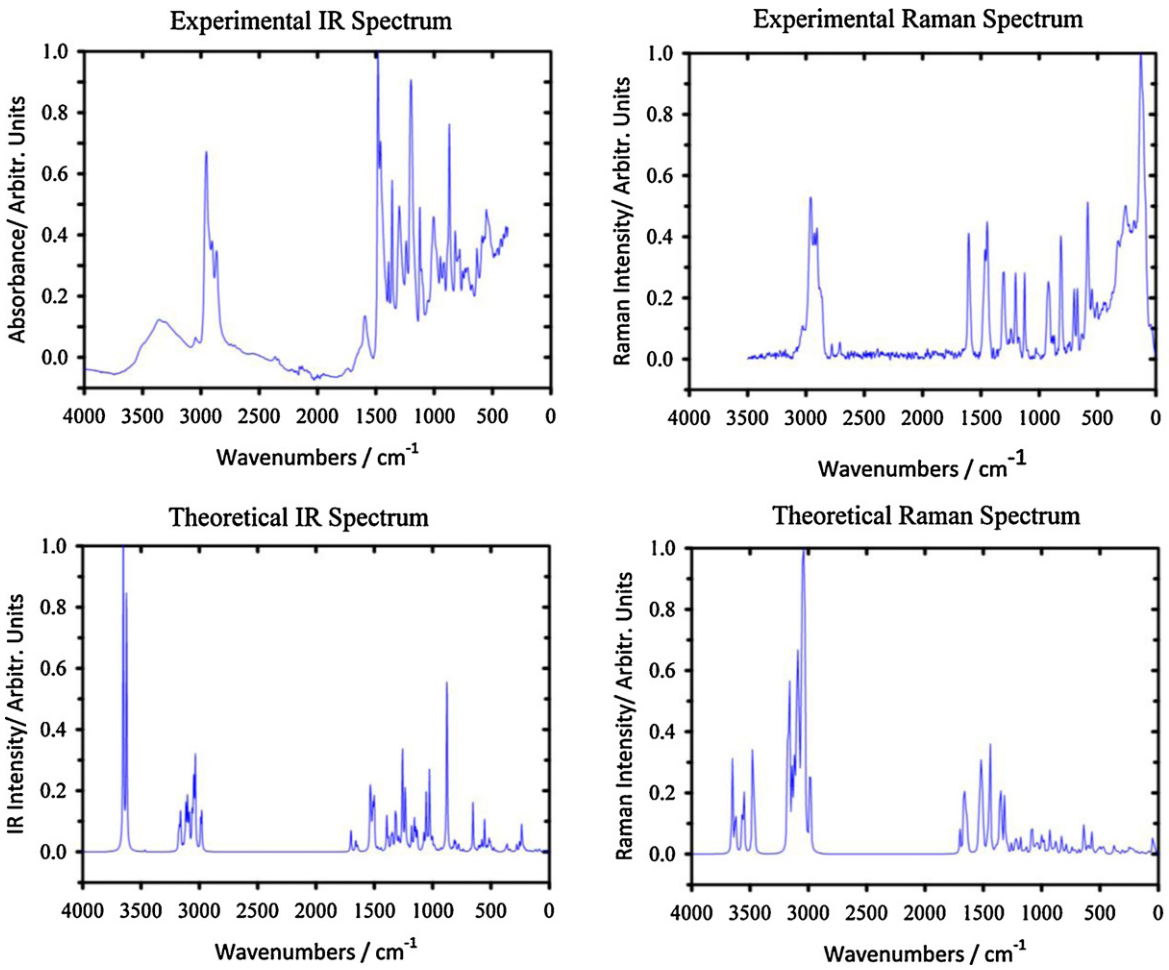

Fig. 2. Experimental and theoretical IR and Raman spectra of 5,11,17,23-Tetra-p-tert-butyl-25,27-bis[aminoethyl]-26-28 dihydroxycalix[4]arene molecule.

The aromatic C—H in-plane bending modes of benzene and its derivatives are observed in the region 1300–1000 cm^{-1}, the bands are sharp but have weak-to-medium intensity. The C–H in-plane bending vibrations predicted at 1387, 1343, 1236, 1233, 1208, 1144, 1123, 1032 and 1000 cm^{-1} by B3LYP/6-31G(d) method show excellent agreement with FT-IR bands at 1388(vw), 1361(m), 1234(w), 1199(vs), 1125(m) and 998(w) cm^{-1}, and FT-Raman bands at 1238(vw), 1198(m), and 1024(vw) cm^{-1}. The same vibrations were observed at 1312w, 1213vw and 1123w cm^{-1} in dispersive Raman spectra with different laser. The aromatic C—H in-plane bending vibrations have substantial overlapping with the ring C—C stretching vibrations. The absorption bands arising from C—H out-of-plane bending vibrations are usually observed in the region at 1000–675 cm^{-1} [29–33]. These vibration modes were observed in

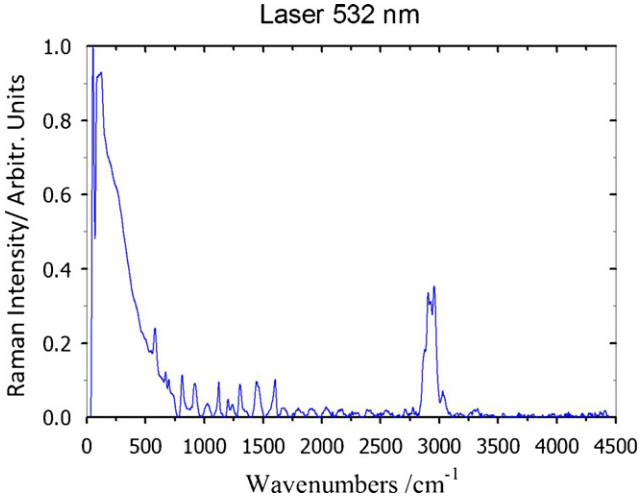

Fig. 3. Experimental dispersive Raman spectra of 5,11,17,23-Tetra-p-tert-butyl-25,27-bis[aminoethyl]-26-28 dihydroxycalix[4]arene molecule (laser 532 nm).

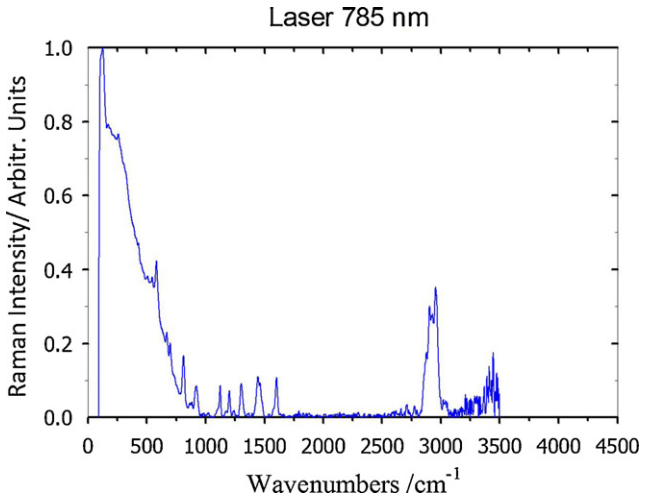

Fig. 4. Experimental dispersive Raman spectra of 5,11,17,23-Tetra-p-tert-butyl-25,27-bis[aminoethyl]-26-28 dihydroxycalix[4]arene molecule (laser 785 nm).

FT-IR spectrum at 869(s), 817(vw), 781(vw) cm^{-1}. This also shows good agreement with theoretically scaled harmonic wavenumber values.

4.2.2. Ring vibrations

The aromatic ring vibrational modes of title compound were analyzed based on the vibrational spectra of previously published vibrations of the benzene molecule are helpful in the identification of the phenyl ring modes [30,32]. The ring stretching vibrations are very prominent, as the double bond is in conjugation with the ring, in the vibrational spectra of benzene and its derivatives [29]. The carbon–carbon stretching modes of the phenyl group are expected in the range from 1650 to 1200 cm^{-1}. The actual position of these modes is determined not so much by the nature of the substituents but by the form of substitution around the ring [34]. In general, the bands are of variable intensity and are observed at 1625–1590, 1590–1575, 1540–1470, 1465–1430 and 1380–1280 cm^{-1} from the wavenumber ranges given by Varsanyi [35] for the five bands in the region. In the present work, the wavenumbers observed in the FT-IR spectrum at 1596(w), 1306(w), 1125(m) cm^{-1} and in FT-Raman spectrum at 1603(s), 1445(s), 1302(ms), 1111(m) and 921(m) cm^{-1} were assigned to C—C stretching vibrations. The same vibrations were observed at 1610(w), 1603(w), 1446(w), 1312(w), 1304(w), 1123(w), 1119(w), 916(w) and 907(w) cm^{-1} in dispersive Raman spectra with different laser. The theoretically computed values in the range 1602–918 cm^{-1} show an excellent agreement with experimental data. These modes are mixed mode with the contribution of C–H in-plane bending vibration in this region. The C—C—C out-of-plane bending modes of the studied molecule is attributed to the low wavenumbers computed at 579, 546, 118 cm^{-1} and these wavenumbers are consistent with the experimental wavenumber 579(w) and 114(s) cm^{-1} in dispersive Raman, 540(vw) and 124(vs) cm^{-1} in FT-Raman spectrum.

4.2.3. Amino group vibrations

The fundamental modes involving the amino group are stretching and bending of NH band, torsion and inversion. It is stated that in amines, the N—H stretching vibrations occur in the region 3500–3300 cm^{-1} [34]. The NH_2 group has two vibrations; one is being asymmetric and other symmetric. The frequency of asymmetric vibration is higher than that of symmetric one. The asymmetric —NH_2 stretching vibration appears from 3500 to 3420 cm^{-1} and the symmetric —NH_2 stretching vibration is observed in the range 3420–3340 cm^{-1}. Based on the above conclusion in our present study, the strong band observed in FT-IR spectrum at 3358(br) cm^{-1}, in FT-Raman at 3328(vw) cm^{-1} and in dispersive Raman spectra at 3315(vw) and 3415(vw) cm^{-1} are assigned to NH_2 symmetric stretching vibrations. The NH_2 symmetric stretching vibrations are computed at 3425, 3411, 3342 and 3328 cm^{-1}. The calculated values are in line with the experimental values and literature data of 3376 cm^{-1} [36]. As evident from Table 2, the TED of these modes are exactly contributing to 99%. The NH_2 torsion can be expected in the low wavenumber range, the wavenumber computed Gaussian 09 and assigned by Gaussview animation package at 268, 245, 229, 228 and 221 cm^{-1} is assigned to NH_2 torsional vibration of the studied molecule (Supp. Mat. Table 1). As indicated by the TED, this mode involves maximum contribution of 33% suggesting that this is mixed with the other modes. The N—H vibrations of present molecule affect the other vibrational modes whereas the N—H vibrations themselves do not get affected by vibrations of other substitutions.

4.2.4. O—H and C—O vibrations

The O—H group vibrations are likely to be the most sensitive to the environment, so they show pronounced shifts in the spectra of the hydrogen-bonded species. The hydroxyl stretching vibrations are generally observed in the region around 3500 cm^{-1} [37]. The O—H band was calculated at 3507, 3480 cm^{-1} (mode no. 246 and 245) for B3LYP/6-31G(d) method. The C—O—H bending vibration is identified at 1580 cm^{-1} by DFT method. This vibration mixes with C—C stretching, and C—C—H bending vibrations as shown in Supp. Mat. Table 1. The C—O stretching vibrations were computed at 1477, 1475, 1474 and 1470 cm^{-1} for the molecule. The wavenumbers predicted in the range 1343–1208 cm^{-1} was assigned to H—C—O and C—O bending vibrations and are in line with the experimental observations.

Table 3
The dipole moments μ (D), the polarizability α (a.u.), the average polarizability α_0 (esu), the anisotropy of the polarizability $\Delta\alpha$ (esu), and the first hyperpolarizability β of 5,11,17,23-Tetra-p-tert-butyl-25,27-bis[aminoethyl]-26-28 dihydroxycalix[4]arene molecule.

μ_x	−0.955526	β_{xxx}	−136.047312
μ_y	0.548448	β_{xxy}	−68.854902
μ_z	0.729598	β_{xyy}	−86.226524
μ_0	1.321416	β_{yyy}	232.800873
α_{xx}	394.011098	β_{xxz}	−38.666965
α_{xy}	29.716489	β_{xyz}	−34.613335
α_{yy}	423.464350	β_{yyz}	−148.487028
α_{xz}	18.525096	β_{xzz}	16.366177
α_{yz}	−12.123668	β_{yzz}	−20.342314
α_{zz}	378.061232	β_{zzz}	−47.182013
α_{total}	59.059512	β_x	−205.907660
$\Delta\alpha$	101.311357	β_y	143.603656
		β_z	−234.336006
		β	29.668586

5. Prediction of polarizability and first hyperpolarizability

The electronic dipole moment (μ_{total}), molecular polarizability (α_{tot}), anisotropy of polarizability ($\Delta\alpha$) and molecular first hyperpolarizability (β_{tot}) of the novel molecular system were investigated using B3LYP/6-31G(d) method, based on the finite-field approach. In the presence of an applied electric field, the energy of a system is a function of the electric field. First hyperpolarizability is a third rank tensor that can be described by $3 \times 3 \times 3$ matrices. The 27 components of the 3D matrix can be reduced to 10 components due to the Kleinman symmetry [38]. It can be given in the lower tetrahedral format. It is obvious that the lower part of the $3 \times 3 \times 3$ matrices is a tetrahedral. The components of β are defined as the coefficients in the Taylor series expansion of the energy in the external electric field. When the external electric field is weak and homogeneous, this expansion becomes:

$$E = E^0 - \mu_\alpha F_\alpha - \tfrac{1}{2}\alpha_{\alpha\beta}F_\alpha F_\beta - \tfrac{1}{6}\beta_{\alpha\beta\gamma}F_\alpha F_\beta F_\gamma - \dots$$

where E_0 is the energy of the unperturbed molecules, F_α is the field at the origin, μ_α, $\alpha_{\alpha\beta}$ and $\beta_{\alpha\beta\gamma}$ are the components of dipole moment, polarizability and the first hyperpolarizability, respectively. The mean polarizability (α), anisotropy of polarizability ($\Delta\alpha$) and the average value of the first hyperpolarizability $\langle\beta\rangle$ can be calculated using the following equations.

$$\alpha_{tot} = \tfrac{1}{3}(\alpha_{xx} + \alpha_{yy} + \alpha_{zz})$$

$$\Delta\alpha = \frac{1}{\sqrt{2}}[(\alpha_{xx} - \alpha_{yy})^2 + (\alpha_{yy} - \alpha_{zz})^2 + (\alpha_{zz} - \alpha_{xx})^2 + 6\alpha_{xz}^2 + 6\alpha_{xy}^2 + 6\alpha_{yz}^2]^{1/2}$$

$$\langle\beta\rangle = [(\beta_{xxx} + \beta_{xyy} + \beta_{xzz})^2 + (\beta_{yyy} + \beta_{yzz} + \beta_{yxx})^2 + (\beta_{zzz} + \beta_{zxx} + \beta_{zyy})^2]^{1/2}$$

In Table 3, the calculated parameters described above and components of electronic dipole moment $\{\mu_i\,(i = x, y, z)$ and total dipole moment $\mu_{tot}\}$ for the studied compound are listed. The total dipole moment can be calculated using the following equation.

$$\mu_{tot} = (\mu_x^2 + \mu_y^2 + \mu_z^2)^{1/2}$$

The polarizability and hyperpolarizability tensors (α_{xx}, α_{xy}, α_{yy}, α_{xz}, α_{yz}, α_{zz} and β_{xxx}, β_{xxy}, β_{xyy}, β_{yyy}, β_{xxz}, β_{xyz}, β_{yyz}, β_{xzz}, β_{yzz},

β_{zzz}) can be obtained by a frequency job output file of Gaussian. However, α and β values of Gaussian output are in atomic units (a.u.) so they have been converted into electronic units (esu) (α; 1 a.u. = 0.1482×10^{-24} esu, β; 1 a.u. = 8.6393×10^{-33} esu).

It is well known that the higher values of dipole moment, molecular polarizability, and hyperpolarizability are important for more active NLO properties. The calculated dipole moment is equal to 1.321416 Debye (D). The highest value of dipole moment is observed for component μ_x. In this direction, this value is equal to 0.955526 D. The calculated polarizability α_{ij} have non-zero values and was dominated by the diagonal components. Total polarizability (α_{tot}) and anisotropy of polarizability ($\Delta\alpha$) were calculated as 59.059512 esu and 101.311357 esu. The first hyperpolarizability value β_{tot} of the compound is equal to $29.668586 \times 10^{-31}$ esu. The hyperpolarizability β dominated by the longitudinal components of β_{xxx}. Domination of particular component indicates on a substantial delocalization of charges in this direction.

Total dipole moment of studied molecule is approximately equal to those of urea (1.373933 D). The polarizability, anisotropy of polarizability and the first hyperpolarizability of title molecule is ca. 15, 12 and 8 times greater than those of urea (α, $\Delta\alpha$ and β of urea are 3.835093 esu, 8.496191 esu, and $3.7346600 \times 10^{-31}$ esu. obtained by B3LYP/6-31G(d,p) method). That is to say, the title compound can be a good candidate of NLO materials.

6. Conclusions

The optimized molecular structures, vibrational frequencies and corresponding vibrational assignments of 5,11,17,23-Tetra-p-tert-butyl-25,27-bis[aminoethyl]-26-28 dihydroxycalix[4]arene have been calculated using B3LYP/6-31G(d) method. Comparison of the experimental and calculated spectra of the molecule showed that DFT-B3LYP method is in good agreement with the experimental data. On the basis of the agreement between the calculated and observed results, assignments of fundamental vibrational modes of 5,11,17,23-Tetra-p-tert-butyl-25,27-bis[aminoethyl]-26-28 dihydroxycalix[4]arene were examined and the complete assignments were proposed. The first hyperpolarizability of studied molecule was found to be ca. 8 times greater than those of urea That is to say, the title compound can be used as a good candidate of NLO materials. This study also demonstrates that scaled DFT/B3LYP calculations are powerful approach for understanding the vibrational spectra of bigger sized organic compounds.

Acknowledgment

This research was supported by Tubitak (Turkish Scientific Association) under project numbers TBAG 109T240.

Appendix A. Supplementary data

Supplementary data associated with this article can be found, in the online version, at http://dx.doi.org/10.1016/j.saa.2012.03.070.

References

[1] J.M. Lehn, Supramolecular Chemistry: Concept and Perspectives, vCH, Weinheim, 1995.
[2] P.D. Beer, P.A. Gale, D.K. Smith, Supramolecular Chemistry, Oxford University Press, Oxford, 1999.
[3] V. Böhmer, Angew. Chem. Int. Ed. Engl. 34 (1995) 713–745.
[4] A. Pochini, R. Ungaro, in: F. Vogtle (Ed.), Comprehensive Supramolecular Chemistry, Pergamon, Oxford, 1996, p. 103.
[5] C.D. Gutsche, in: J.F. Stoddart (Ed.), Monographs in Supramolecular Chemistry, RSC, Cambridge, 1998.
[6] A. Ikeda, S. Shinkai, Chem. Rev. 97 (1997) 1713–1734.
[7] S. Houmadi, D. Coquière, L. Legrand, M.C. Fauré, M. Goldmann, O. Reinaud, S. Rémita, Langmuir 23 (2007) 4849–4855.
[8] T.D. Chung, J. Park, J. Kim, H. Lim, M.J. Choi, J.R. Kim, S.K. Chang, H. Kim, Anal. Chem. 73 (2001) 3975–3980.
[9] M. Giannetto, G. Mori, A. Notti, S. Pappalardo, M.F. Parisi, Chem. Eur. J. 7 (2001) 3354–3362.
[10] C.D. Gutsche, in: J.F. Stoddart (Ed.), Monographs in Supramolecular Chemistry, RSC, Cambridge, 1989.
[11] A. Suwattanamala, A.L. Magalhaes, J.A.N.F. Gomes, Chem. Phys. 310 (2005) 109–122.
[12] K. Kim, S.J. Park, J.I. Choe, Bull. Korean Chem. Soc. 29 (2008) 1893–1902.
[13] I. Kara, H.H. Kart, N. Kolsuz, O.O. Karakus, H. Deligoz, Struct. Chem. 20 (2009) 113–119.
[14] D.L. Cao, F. Ren, Y. Feng, S. Liu, S. Chen, J. Mol. Model. 16 (2010) 589–595.
[15] Y. Liu, G. Huang, H.Y. Zhang, J. Mol. Struct. 608 (2002) 213–217.
[16] H.K. Lee, H. Yeo, D.H. Park, S. Jeon, Bull. Korean Chem. Soc. 24 (2003) 1737–1741.
[17] M. Bayrakci, S. Ertul, O. Sahin, M. Yilmaz, J. Incl. Phenom. Macrocycl. Chem. 63 (2009) 241–247.
[18] P.V. Kolinsky, Opt. Eng. 31 (1992) 1676–1684.
[19] D.F. Eaton, Science 253 (1991) 281–287.
[20] M.J. Frisch, et al., Gaussian 09, Revision A.1, Gaussian, Inc., Wallingford, CT, 2009.
[21] H.B. Schlegel, J. Comput. Chem. 3 (1982) 214–218.
[22] M.J. Frisch, A.B. Nielsen, A.J. Holder, Gauss View Users Manual, Gaussian Inc., Pittsburgh, PA, 2000.
[23] F. Weinhold, J. Am. Chem. Phys. Soc. 102 (1980) 7211–7218, GAUSS VIEW.
[24] M.H. Jamroz, Vibrational Energy Distribution Analysis, VEDA 4 Computer Program, Poland, 2004.
[25] G. Keresztury, S. Holly, J. Varga, G. Besenyei, A.Y. Wang, J.R. Durig, Spectrochim. Acta 9A (1993) 2007–2026.
[26] G. Keresztury, J.M. Chalmers, P.R. Griffith, Raman Spectroscopy: Theory, Handbook of Vibrational Spectroscopy, vol. 1, John Wiley & Sons Ltd., New York, 2002.
[27] V.K. Rastogi, M.A. Palafox, R.P. Tanwar, L. Mittal, Spectrochim. Acta A 58 (2002) 1987–2004.
[28] M. Silverstein, G.C. Basseler, C. Morill, Spectrometric Identification of Organic Compounds, Wiley, New York, 1981.
[29] G. Varsanyi, Vibrational Spectra of Benzene Derivative, Academic Press, New York, 1969.
[30] N.B. Colthup, L.H. Daly, S.E. Wiberley, Introduction to Infrared and Raman Spectroscopy, Academic Press, New York, 1990.
[31] F.R. Dollish, W.G. Fateley, F.F. Bentley, Characteristic Raman Frequencies of Organic Compounds, John Wiley & Sons, New York, 1997.
[32] G. Socrates, Infrared Characteristic Group frequencies, Wiley-Interscience Publication, New York, 1980.
[33] B. Smith, Infrared Spectral Interpretation, A Systematic Approach, CRC Press, Washington, DC, 1999.
[34] L.J. Bellamy, The Infrared Spectra of Complex Molecules, 3rd ed., Wiley, New York, 1975.
[35] G. Varsanyi, Assignments of Vibrational Spectra of Seven Hundred Benzene Derivatives, vols. 1–2, Adam Hilger, 1974.
[36] B.B. Ivanova, Spectrochim. Acta 62A (2005) 58–65.
[37] D. Sajan, I. Hubert Joe, V.S. Jayakumar, J. Zaleski, J. Mol. Struct. 785 (2006) 43–53.
[38] D.A. Kleinman, Phys. Rev. 126 (1962) 1977–1979.